Analytical Biochemistry 415 (2011) 32–38

Contents lists available at ScienceDirect

Analytical Biochemistry

journal homepage: www.elsevier.com/locate/yabio

Intracellular anion fluorescence assay for sodium/iodide symporter substrates

Julie Di Bernardo, Carmela Iosco, Kerry J. Rhoden *

Medical Genetics Unit, Department of Gynecologic, Obstetric, and Pediatric Sciences, University of Bologna, Bologna 401 38, Italy

ARTICLE INFO

Article history:
Received 22 December 2010
Received in revised form 12 April 2011
Accepted 12 April 2011
Available online 20 April 2011

Keywords:
Fluorescence microscopy
Biosensor
Intracellular concentration
Yellow fluorescent protein
Anions
Thiocyanate
Nitrate
Chlorate
Perchlorate
Perrhenate
Thyroid gland

ABSTRACT

The sodium/iodide symporter (NIS) is primarily responsible for iodide accumulation in the thyroid gland for the synthesis of thyroid hormones; however, it can also transport other lyotropic anions in the thyroid gland and nonthyroid tissues. Some NIS substrates have important physiological or clinical roles, and others are environmental contaminants with health-related consequences. The aim of this study was to assess the utility of a yellow fluorescent protein variant, YFP–H148Q/I152L, as a biosensor to monitor the cellular uptake of NIS substrates, including thiocyanate (SCN^-), nitrate (NO_3^-), chlorate (ClO_3^-), perchlorate (ClO_4^-), and perrhenate (ReO_4^-). The fluorescence of purified YFP–H148Q/I152L was suppressed by anions with an order of potency of $ReO_4^- > ClO_4^- = I^- = SCN^- = ClO_3^- > NO_3^- \gg Cl^-$. Anions also suppressed the fluorescence of YFP–H148Q/I152L expressed in FRTL-5, a thyroid cell line with high NIS expression. Quantitation of intracellular concentrations revealed differences among anions in the affinity and maximal velocity of NIS-mediated uptake as well as in the rate constant for passive efflux. These results suggest that YFP–H148Q/I152L can serve as an intracellular biosensor of NIS-transported anions and may be useful to study the physiology of endogenous anions as well as the health-related consequences of environmental anions.

Fluorescent proteins are increasingly used as genetically encodable biosensors to monitor the chemical dynamics of living cells. Green fluorescent protein (GFP)[1]-based biosensors have been used to monitor real-time changes in the concentration of specific intracellular analytes in response to physiological, pharmacological, and pathological perturbations. Yellow-shifted variants of GFP are sensitive to halides and have been used to monitor changes in their intracellular concentration, to identify and characterize the proteins involved in their transport and to screen for drugs to treat defective anion transport in human disease [1–7].

The sodium/iodide symporter (NIS) is primarily known as the transporter responsible for the accumulation of iodide in the thyroid gland for the synthesis of thyroid hormones [8]. Although iodide is its major substrate, NIS is also able to transport other anions of the Hofmeister or lyotropic series, with weakly hydrated chaotropic anions having the greatest affinity. NIS substrates include pseudohalides such as thiocyanate and other monovalent anions such as nitrate, chlorate, perchlorate, and perrhenate [9,10]. These anions are concentrated by the thyroid gland and/or compete with iodide uptake, whereas other common anions such as phosphate and sulfate are not thyroid substrates [11,12]. NIS is also expressed in other tissues such as the stomach, salivary glands, lactating mammary gland, and placenta, where it may contribute to the extrathyroidal transport of iodide and other substrates [8].

Some NIS substrates, such as thiocyanate and nitrate, are normally present in the circulation, and elevated plasma levels reflect increased dietary consumption or environmental exposure. Endogenous thiocyanate results from the metabolism of plant-derived thioglucosides and plays a physiological role in the innate host defense system of epithelial barriers following conversion by peroxidase into antimicrobial metabolites [13]. Tobacco smoking elevates plasma thiocyanate levels through the hepatic detoxification of cyanide [14]. Nitrate is endogenously generated as the end product of nitric oxide metabolism and is present in the diet as a natural component of vegetables and as a food additive. The entero-salivary recycling of dietary nitrate produces nitrite and nitric oxide that regulate important physiological functions [15]. The increased use of nitrate-containing fertilizers and the emission of nitrogen-containing compounds by industries and automobiles have led to drinking water contamination and increased nitrate consumption [16]. Chlorate and perchlorate are also industrial pollutants, and their presence in the body reflects intake of contaminated foodstuffs and water [17,18]. Concern has been raised over potential health effects of environmental NIS substrates because these anions compete with and inhibit the uptake of iodide by the thyroid

* Corresponding author. Fax: +39 051 2088416.
E-mail address: kerry.rhoden@unibo.it (K.J. Rhoden).

[1] *Abbreviations used:* GFP, green fluorescent protein; NIS, sodium iodide symporter; YFP, yellow fluorescent protein; GST, glutathione *S*-transferase; PBS, phosphate-buffered saline; HBS, Hepes-buffered solution; PBPK, physiologically based pharmacokinetic.

0003-2697/$ - see front matter © 2011 Elsevier Inc. All rights reserved.
doi:10.1016/j.ab.2011.04.017

gland, and chronic exposure may disrupt thyroid function in susceptible individuals [19]. The presence of NIS at extrathyroidal sites [8] also suggests that the consequences of NIS-mediated transport of environmental anions may extend beyond the thyroid gland.

NIS substrates also have a clinical utility. Radioactive iodide (^{131}I) has long been used to visualize and treat thyroid cancer, and other NIS-transported radioisotopes with enhanced local emission and shorter half-lives, such as ^{99m}Tc-pertechnetate, ^{188}Re-perrhenate, and ^{211}At-astatine, are emerging as alternative radionuclides for NIS-based nuclear imaging and radiotherapy [20,21].

Cellular ions can be detected with chemical assays, radiotracers, electrophysiological techniques, and optical sensors, and several of these techniques have been used to detect NIS-mediated anion transport in thyroid and nonthyroid cells. Radionuclides, in particular, have been invaluable in identifying and characterizing NIS activity, specifically with regard to the transport of iodide, perrhenate, and pertechnetate [9,22–24]. The ability of NIS to transport other substrates has been inferred from the measurement of ionic currents induced by anions in NIS-expressing cells [10], and perchlorate accumulation in thyroid cells has been demonstrated chemically by ion chromatography–mass spectrometry [25]. To date, however, no single technique is capable of measuring the cellular accumulation of different NIS substrates.

Previously, we developed a cell-based assay of iodide transport by NIS using YFP–H148Q/I152L, a halide-sensitive variant of yellow fluorescent protein (YFP) [26,27]. YFP–H148Q/I152L's fluorescence is quenched by iodide, and the protein can be transiently or stably expressed in cells to monitor dynamic changes in intracellular iodide concentration. In addition, YFP–H148Q/I152L is sensitive to perchlorate, allowing the detection of perchlorate uptake by NIS-expressing cells [28]. The aim of the current study was to determine the sensitivity of YFP–H148Q/I152L to other NIS substrates, including thiocyanate, nitrate, chlorate, and perrhenate, and to use it to monitor and quantify the intracellular accumulation of these anions by NIS-expressing cells.

Materials and methods

Expression and purification of recombinant YFP–H148Q/I152L

Recombinant YFP–H148Q/I152L was expressed in bacteria and purified as described previously [26]. Briefly, BL21(DE3) bacteria were transformed with a pGEX-4T-1 vector (GE Healthcare) containing the YFP–H148Q/I152L open reading frame in frame with the glutathione *S*-transferase (GST) gene. Protein production was induced with 0.5 mM isopropyl-β-D-1-thiogalactopyranoside for 5 h. Bacteria were lysed in phosphate-buffered saline (PBS, 50 mM, pH 7.4) containing 1% Nonidet P-40 (NP-40), 5 mM ethylenediaminetetraacetic acid (EDTA), 0.4 mg/ml lysozyme, and protease inhibitors (Complete Roche inhibitor cocktail). The GST–YFP–H148Q/I152L fusion protein was purified by glutathione agarose affinity chromatography and eluted in a chloride-free solution consisting of 50 mM sodium phosphate (pH 8.8), 25 mM reduced free glutathione, and 200 mM sodium gluconate.

Cell culture

Cellular uptake studies were performed on FRTL-5, a highly differentiated thyroid follicular cell line derived from normal Fischer rats [29]. Cells were cultured in Coon's modified F12 medium supplemented with 5% newborn calf serum, 1 μg/ml insulin, 3.6 ng/ml hydrocortisone, 5 μg/ml apotransferrin, 10 ng/ml Gly-His-Lys acetate, 10 ng/ml somatostatin, 1 mU/ml thyroid stimulating hormone (TSH), 100 U/ml penicillin, and 100 μg/ml streptomycin. Cells were passaged with Ca^{2+}- and Mg^{2+}-free Hank's balanced salt solution containing 20 U/ml collagenase, 0.75 mg/ml trypsin, and 2% dialyzed chicken serum. An FRTL-5 cell line with stable expression of YFP–H148Q/I152L was previously generated through liposome-mediated transfection with a pcDNA3.1 vector containing YFP–H148Q/I152L complementary DNA (cDNA) and selection by antibiotic resistance [26].

Fluorescence microscopy

YFP–H148Q/I152L fluorescence was monitored with a Zeiss Axiovert 200 inverted microscope equipped with a 40× oil immersion objective, an XBO Xenon 75 W short arc lamp, a Lambda 10C filter changer (Sutter Instrument, Crisel Instruments, Rome, Italy), and an XF104-2 YFP filter set for excitation at 500 ± 12.5 nm and emission at 545 ± 17.5 nm (Omega Optical, Crisel Instruments). Images were acquired with a CoolSNAP HQ charge-coupled device (CCD) camera (Roper Scientific, Crisel Instruments), and fluorescence intensity was quantified with MetaFluor software (Universal Imaging, Crisel Instruments).

YFP–H148Q/I152L calibration

The anion sensitivity of YFP–H148Q/I152L fluorescence was determined with purified recombinant protein. Purified protein was suspended in a buffer consisting of 50 mM sodium phosphate buffer (pH 7) and 300 mM sodium gluconate. Specific anion concentrations were achieved by substituting gluconate with 0.01–300 mM iodide, thiocyanate, perchlorate, nitrate, chlorate, or perrhenate on an equimolar basis. Fluorescence intensity was quantified in 8-μl aliquots of the YFP–H148Q/I152L-containing solution deposited on a coverslip in triplicate.

Affinity constants (K_a) were determined by nonlinear regression using the four-parameter logistic equation $F = F_{min} + (F_{max} - F_{min})/(1 + 10\exp(\log K_a - \log[X])n)$, where F is the fluorescence at each anion concentration ([A]), F_{max} is the maximal fluorescence in the absence of anions, F_{min} is the residual fluorescence in the presence of saturating concentrations of anions, K_a is the anion concentration causing a 50% of maximal decrease in fluorescence, and n is the Hill slope. Curve fitting was performed with GraphPad Prism (GraphPad Software, San Diego, CA, USA).

Cellular uptake studies

Cellular YFP–H148Q/I152L fluorescence was monitored in cells adhered to coverslips and maintained in a thermostatically controlled imaging chamber (Warner Instruments). Cells were perfused at 4–5 ml/min at 37 °C with PBS consisting of 137 mM NaCl, 2.7 mM KCl, 0.7 mM $CaCl_2$, 1.1 mM $MgCl_2$, 1.5 mM KH_2PO_4, 8.1 mM Na_2HPO_4, and 10 mM glucose (pH 7.4). Anion influx was initiated by exposing cells to PBS containing 1–1000 μM of the respective anions for 5 min. The sodium dependence of anion influx was examined in a Hepes-buffered solution (HBS) containing 10 mM Hepes (pH 7.4), 145 mM NaCl, 5 mM KCl, 0.7 mM $CaCl_2$, 1.1 mM $MgCl_2$, and 10 mM glucose. Low-Na^+ HBS containing 10 mM Na^+ was prepared by replacing NaCl with equimolar choline chloride.

Average fluorescence intensity was quantified within a selected region of interest containing 30–100 cells. Baseline fluorescence (in PBS) was fitted by nonlinear regression to a third-order polynomial equation to correct for fluorescence decay due to photobleaching and spontaneous changes in resting cellular fluorescence that may occur over prolonged periods of time. Fluorescence at each time point (F) was normalized to the fitted baseline fluorescence (F_0) to give a measure of relative fluorescence (RF, where $RF = F/F_0$) in the presence of extracellular NIS substrates. Intracellu-

lar anion concentrations ($[A^-]i$) were calculated according to the equation $[A^-]i = K_a(RF_{max} - RF)/(RF - RF_{min})$, where RF is the normalized fluorescence at each extracellular anion concentration, RF_{max} is fluorescence in the absence of anions (defined as 1), RF_{min} is fluorescence in the presence of saturating concentrations of anions, and K_a is the affinity constant of YFP–H148Q/I152L for anions. The limit of detection of intracellular anions was defined as the concentration producing a fluorescence decrease of 3 times the standard deviation (3 × SD) of the baseline fluorescence. During exposure to anions, intracellular anion concentrations were fit over time to a one- or two-phase exponential association equation, and the maximal rate of anion influx (in μM/s) was obtained from the derivative of the best fit curve. The relationship between influx rate and extracellular concentration was analyzed according to the Michaelis–Menten equation to derive K_m and V_{max} values for the uptake of each NIS substrate. Following anion exposure, cells were rinsed with PBS to monitor the recovery of resting fluorescence, and anion efflux rate constants were determined by fitting intracellular concentrations over time to a one- or two-phase exponential decay function. Curve fitting was performed with GraphPad Prism.

Results and discussion

Anion sensitivity of purified YFP–H148Q/I152L

The sensitivity of YFP–H148Q/I152L to anions was first analyzed in solution using purified YFP–H148Q/I152L produced in bacteria. YFP–H148Q/I152L fluorescence was quenched by anions with more than 90% maximal suppression occurring within 1–2 s of anion addition (except Cl^-, which did not reach its maximal effect at the highest concentration tested). Fluorescence quenching was concentration dependent, with data fitting well to a single site binding model with Hill slopes close to −1. The order of potency of anions was $ReO_4^- > ClO_4^- = I^- = SCN^- = ClO_3^- > NO_3^- > Cl^-$ (Fig. 1 and Table 1). The fluorescence of another YFP variant, YFP–H148Q, is also decreased by anions with a similar order of potency of $ClO_4^- = I^- > SCN^- > NO_3^- > Cl^-$, albeit with up to 10-fold lower affinities [30]. The order of potency is consistent with binding of weakly hydrated chaotropic anions. Anions suppress the fluorescence of YFPs by static quenching following ground state binding to a site close to the Ser65, Tyr66, and Gly67 tri-amino acid chromophore [30,31]. Anion binding alters the electrostatic environment of the chromophore, promoting protonation and a change in apparent pK_a. The anion selectivity of YFP variants is related to hydration forces, with protein interaction generally increasing with decreasing hydration energy. Furthermore, the electrostatic configuration of polyatomic anions, such as perchlorate and thiocyanate, may improve binding interactions with several protein groups close to the chromophore [31].

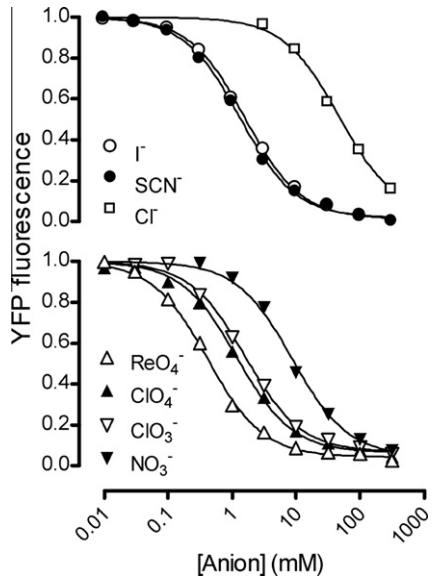

Fig.1. Anion sensitivity of YFP–H148Q/I152L fluorescence. Purified YFP–H148Q/I152L was incubated in phosphate buffer containing anions (I^-, Cl^-, SCN^-, NO_3^-, ClO_3^-, ClO_4^-, and ReO_4^-), and fluorescence was expressed relative to that in the absence of anions. Fluorescence data were fitted by nonlinear regression to a four-parameter logistic equation. Data points represent the means ± standard errors of six measurements.

Table 1
Anion sensitivity of YFP–H148Q/I152L fluorescence.

	$K_{0.5}$ (mM)	Maximal fluorescence decrease (%)	Hill slope
ReO_4^-	0.4	96	−1.06
ClO_4^-	1.2	95	−0.91
SCN^-	1.3	98	−0.96
I^-	1.6	99	−0.94
ClO_3^-	1.6	93	−1.01
NO_3^-	7.9	93	−1.15
Cl^-	4.6	N.D.	−1.15

Best fit values are derived by nonlinear regression fitting of fluorescence data to a four-parameter logistic equation. $K_{0.5}$ is the anion concentration causing a half-maximal decrease in YFP–H148Q/I152L fluorescence. Data represent best fit values of six fluorescence measurements at each anion concentration. N.D., not determined.

Anion sensitivity of cellular YFP–H148Q/I152L

The utility of YFP–H148Q/I152L as an intracellular anion biosensor was examined in FRTL-5 rat thyroid cells. These cells have a high endogenous expression of NIS, and uptake via this transporter results in a more than 30-fold concentration of iodide within cells with respect to the extracellular medium [23,29,32].

Exposure of FRTL-5 cells with stable YFP–H148Q/I152L expression to extracellular anions (I^-, SCN^-, NO_3^-, ClO_3^-, ReO_4^-, and ClO_4^-) resulted in a time- and concentration-dependent decrease in cellular fluorescence (Fig. 2). Fluorescence decreased within 10 s of anion exposure, and responses were maximal or near maximal within 5 min. Fluorescence changes were fully reversible on rinsing with PBS, and repeated exposure produced reproducible responses. Anions differed in the magnitude of fluorescence changes induced; thus, exposure of FRTL-5 cells to 1 mM anions decreased cellular fluorescence by 10% in the case of perrhenate and perchlorate, 25% in the case of thiocyanate and nitrate, 50% in the case of iodide, and 70% in the case of chlorate. It is unlikely that the magnitude of responses reflects differences in the ability of anions to interact with the fluorochrome given that the same anion concentration (1 mM) suppressed the fluorescence of purified YFP–H148Q/I152L by 10% in the case of nitrate, by 40% in the case of iodide, thiocyanate, chlorate, and perchlorate, and by 70% in the case of perrhenate. Thus, the different effects of anions on cellular versus purified YFP–H148Q/I152L fluorescence presumably reflect differences in anion uptake by cells. Anion-induced changes in cellular YFP fluorescence were prevented by reducing the extracellular concentration of Na^+ from 145 to 10 mM (data not shown), consistent with the Na^+ dependence of NIS. Furthermore, anions had no effect on intracellular pH measured with 2,7-bis(2-carboxyethyl)-5(6)-carboxyfluorescein (BCECF) (data not shown), indicating that changes in cellular YFP–H148Q/I152L fluorescence are not indirectly due to changes in intracellular pH.

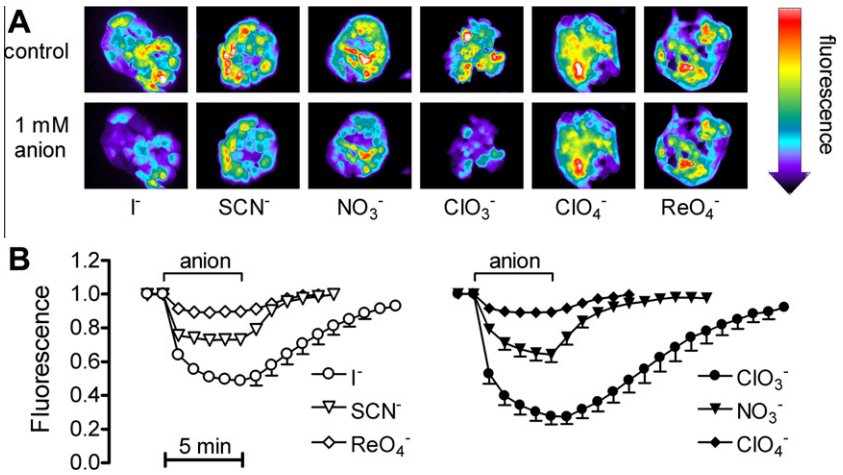

Fig.2. Anion-Induced changes in YFP–H148Q/I152L fluorescence in FRTL-5 thyrocytes. (A) Fluorescence photomicrograph of cells exposed for 5 min to 1 mM anions, with fluorescence intensity shown in a pseudocolor scale. (B) Time course of fluorescence changes during exposure to 1 mM anions. Fluorescence intensity at each time point was normalized against resting fluorescence in the absence of anions. Data points represent means ± standard errors of 8–12 measurements.

Intracellular anion quantification

Intracellular anion concentrations were estimated from anion-induced changes in cellular fluorescence using the measured affinity of purified YFP–H148Q/I152L (Fig. 3). The limit of detection of intracellular anions, defined as the concentration producing a fluorescence decrease of 3 times the standard deviation of baseline fluorescence ($3 \times SD = 2.1\%$, $n = 100$), was 9 μM for perrhenate, 27 μM for perchlorate, 34 μM for iodide, 29 μM for thiocyanate, 37 μM for chlorate, and 196 μM for nitrate. All anions were concentrated within cells to above their extracellular concentration, consistent with NIS-mediated transport driven by the inward electrochemical gradient for Na^+. Minimum extracellular anion concentrations leading to detectable intracellular levels were 0.3 μM perrhenate, 1 μM perchlorate and iodide, 3 μM thiocyanate, 30 μM nitrate, and 30 μM chlorate.

The quantitation of intracellular anions depends on the adequacy of the measured affinity of YFP–H148Q/I152L for anions. The anion sensitivity of YFP variants is influenced by pH, with acidification increasing sensitivity and alkalinization decreasing sensitivity [27,31]. In this study, YFP–H148Q/I152L calibration was carried out at a pH value of 7.0, equivalent to the intracellular pH of FRTL-5 cells [27]. Furthermore, in a cellular environment, NIS substrates may need to compete with other biologically active anions for binding to YFP–H148Q/I152L. The major intracellular anion is Cl^-, which is present in thyroid cells at a concentration of approximately 15 mM [27,33]. YFP–H148Q/I152L sensitivity to anions was not altered by 15 mM Cl^- (data not shown), suggesting that, in the current study at least, intracellular Cl^- is unlikely to affect anion quantitation. Other biologically active anions include phosphate, carbonate, and sulfate; however YFPs are insensitive to these anions [30,34]. Competition with other unidentified anions cannot be excluded and could lead to an underestimate of the intracellular concentration of NIS substrates. Quantitation of anion uptake under conditions of altered intracellular pH or Cl^- concentration, or in other cell types, will require biosensor calibration in an appropriate ionic environment.

Anion transport kinetics

The rate of change of intracellular anion concentrations was used to estimate kinetic parameters of transport (K_m, V_{max}, and V_{max}/K_m). Anion uptake was saturable with respect to extracellular concentration and conformed to Michaelis–Menten kinetics (Fig. 4 and Table 2). The order of affinity of anions for uptake was $ReO_4^- \geqslant ClO_4^- \gg I^- = SCN^- \gg ClO_3^- \geqslant NO_3^-$; thus, perrhenate and perchlorate have a 10-fold higher affinity than iodide, thiocyanate has a similar affinity, and chlorate and nitrate have a 10- to 20-fold lower affinity. The order of affinity is unlikely to reflect differences in the affinity of substrates for YFP–H148Q/I152L because chlorate and perchlorate, for instance, have identical affinities for purified YFP–H148Q/I152L but have very different effects on cellular fluorescence in terms of both the magnitude of the response and its concentration dependence.

The affinity of NIS for its substrates has previously been studied with radiotracers and electrophysiological techniques. Radiotracer uptake by NIS-expressing cells provides a direct measure of transport affinity and has yielded estimates of 30 μM for iodide using ^{125}I and 4 μM for perrhenate using $^{186}ReO_4^-$ [23,32,35,36]. The affinities of other substrates has been determined indirectly according to their ability to induce transmembrane currents (due to the electrogenic nature of NIS-mediated transport) or to inhibit radioiodide uptake in NIS-expressing cells. Using these methods, substrate affinities were determined to be approximately 1 μM for perchlorate and perrhenate, 20–100 μM for thiocyanate, and in the range of 0.1–1 mM for chlorate and nitrate [9,10,37]. Our own estimates of substrate affinity are in line with these values and provide a more direct measure of transport affinity. The mechanistic basis for the transport selectivity of NIS is unclear but may be related to the size, shape, and hydration energy of anions [12,38]. NIS substrates belong to the lyotropic or Hofmeister series that ranks ions according to their effects on protein solubility, with weakly hydrated chaotropic anions exhibiting a higher affinity for NIS.

The maximal rate of anion transport (V_{max}) exhibited a rank order of $NO_3^- = ClO_3^- \gg I^- > SCN^- \gg ClO_4^- > ReO_4^-$, with lower affinity anions exhibiting higher V_{max} values. Intracellular anion concentrations generally correlated with V_{max} values for uptake; thus, nitrate and chlorate exhibited the highest V_{max} values and resulted in the highest intracellular concentrations (albeit at high extracellular concentrations), whereas perrhenate and perchlorate exhibited the lowest V_{max} values and produced the lowest intracellular concentrations (but at low extracellular concentrations). Significantly, iodide, perrhenate, and perchlorate showed the greatest intracellular-to-extracellular concentration ratios, and this may reflect the greater transport efficiency of NIS for these ions (V_{max}/K_m ratio). The high transport efficiency of perrhenate is particularly relevant for the application of perrhenate radioisotopes in nuclear

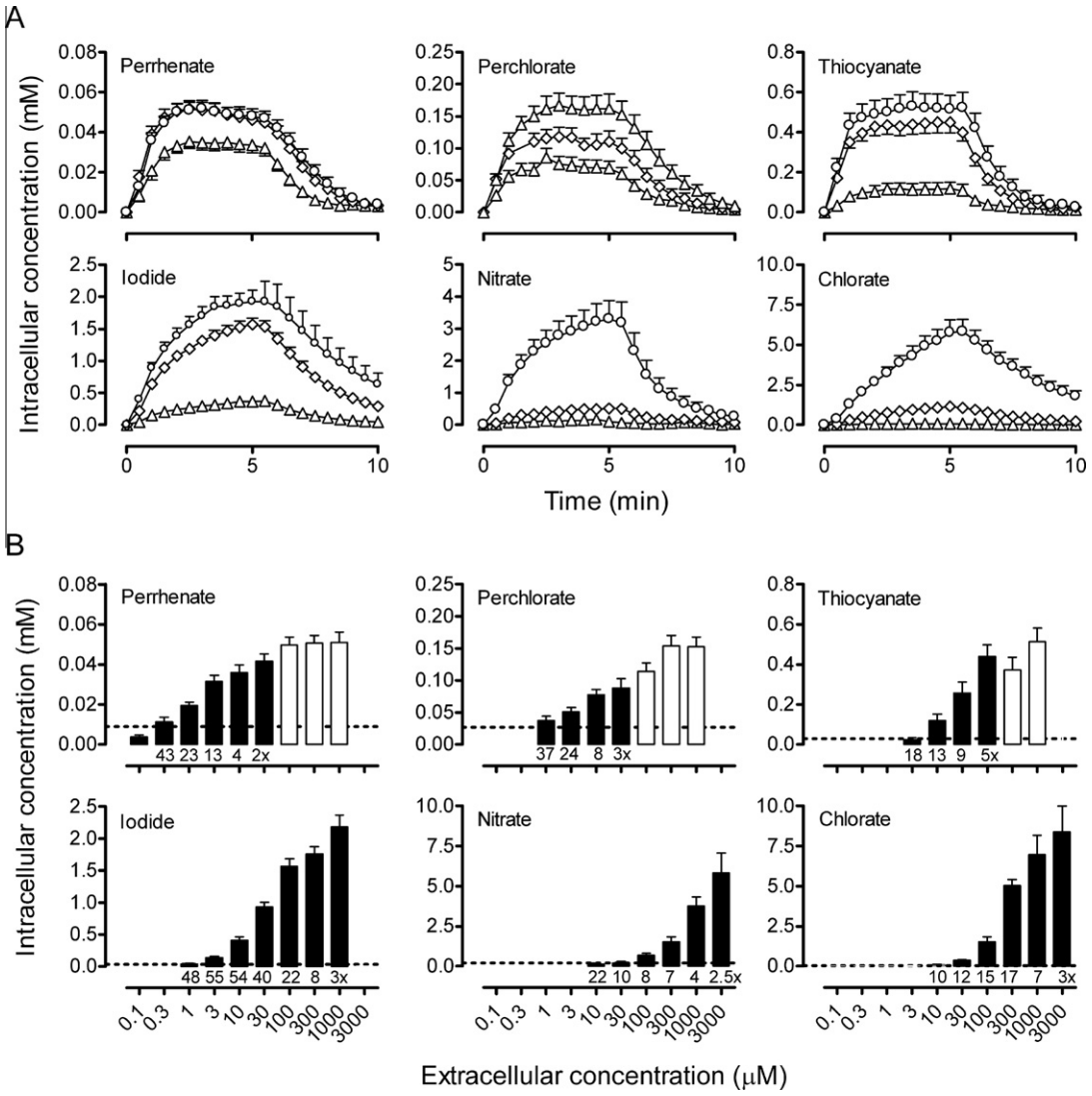

Fig.3. Accumulation of NIS substrates in FRTL-5 cells. (A) Time course of anion uptake. (B) Maximal intracellular concentration during exposure of cells to extracellular anions, estimated by nonlinear regression fitting of time course data in panel A to a one- or two-phase exponential association equation. Numbers beneath bars represent the intracellular-to-extracellular concentration ratios (*IC*/*EC*); filled bars represent *IC*/*EC* > 1, and white bars represent *IC*/*EC* ⩽ 1. The horizontal dashed line represents the limit of detection for intracellular anions. Data points or bars represent means ± standard errors of 8 to 12 measurements.

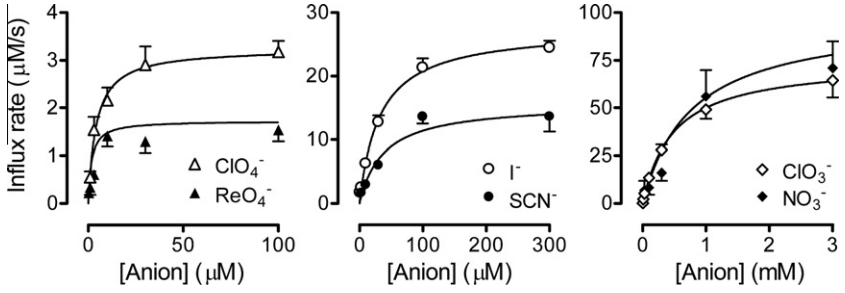

Fig.4. Michaelis–Menten kinetic analysis of anion uptake by FRTL-5 cells. The maximal rate of anion uptake is plotted as a function of extracellular anion concentration. Data points represent means ± standard errors of 8–12 measurements.

medicine, allowing low doses to be used *in vivo* to image NIS-expressing tumors.

Following NIS-mediated uptake, anions rapidly diffuse out of cells along their electrochemical gradient. Intracellular anion concentrations, therefore, reflect the balance of influx and efflux, and differences in membrane permeability to different anions may contribute to the observed differences in steady-state anion accumulation. Anion efflux was monitored during the recovery of resting fluorescence following exposure to anions and subsequent washing with PBS. Michaelis–Menten parameters for efflux could not be compared because saturation of the efflux rate with respect to intracellular anion concentration was not achieved for some

Table 2
Kinetic parameters for anion uptake by FRTL-5 thyrocytes.

	K_m (μM)	V_{max} (μM/s)	V_{max}/K_m (s^{-1})
ReO_4^-	1.9 ± 0.7	1.7 ± 0.1	0.91
ClO_4^-	3.9 ± 1.0	3.2 ± 0.2	0.82
I^-	33 ± 6	28 ± 1	0.84
SCN^-	38 ± 11	16 ± 1	0.41
ClO_3^-	486 ± 112	74 ± 6	0.15
NO_3^-	770 ± 314	98 ± 25	0.13

V_{max}/K_m, efficiency of transport. Kinetic parameters (K_m and V_{max}) represent means ± standard errors of 8–12 experiments.

anions. Instead, efflux rate constants were measured and yielded a rank order of $SCN^- > ClO_4^- = ReO_4^- > NO_3^- = I^- > ClO_3^-$. Thus, efflux rate constants for thiocyanate (0.0159 s^{-1}), perchlorate (0.0132 s^{-1}), and perrhenate (0.0121 s^{-1}) were significantly higher than that for iodide (0.0088 s^{-1}) ($P < 0.01$, Dunnett's multiple comparison test), suggesting that membrane permeability to these three anions is greater than that to iodide and that this limits their steady-state accumulation. In contrast, the efflux rate constant for chlorate (0.0058 s^{-1}) was significantly lower than that for iodide ($P < 0.01$, Dunnett's multiple comparison test), and this contributes to a greater chlorate accumulation, albeit at extracellular concentrations that are much higher than can be achieved *in vivo* through environmental contamination.

An important caveat to the use of YFP-H148Q/I152L to compare anion fluxes is that transport kinetics may be obscured by differences in the kinetics of anion binding to YFP–H148Q/I152L. Chloride binding to YFP–H148Q/I152L occurs with association/dissociation time constants of approximately 50 ms [1], which would not be expected to affect estimates of anion fluxes. Time constants for the binding of other anions have not been measured; however, fluorescence quenching of purified YFP–H148Q/I152L was complete within 1–2 s of anion addition, suggesting that anion binding to the chromophore does not limit fluorescence responses of intact cells.

Conclusion

Genetically encoded fluorescent proteins such as YFP–H148Q/I152L represent powerful tools to probe the internal milieu of cells. The current study demonstrates the utility of YFP–H148Q/I152L as an intracellular biosensor to monitor the cellular uptake of diverse NIS substrates, not previously possible with other techniques. YFP–H148Q/I152L enables real-time monitoring of intracellular anion concentrations in single cells, representing a distinct advantage over chemical, radiotracer, and electrophysiological techniques. The kinetic parameters derived in this study may be useful for physiologically based pharmacokinetic (PBPK) modeling of anion distribution in the body to better assess the potential consequences of environmental exposure. PBPK models have been developed to assess iodide and perchlorate distribution in the body [39] and will be useful to assess the distribution of other NIS substrates. In the current study, intracellular anion concentrations were measured in FRTL-5 thyrocytes as a model of NIS-expressing cells; however, the biosensor may be applied to other cell types that normally express NIS to study its role in extrathyroidal anion transport. Measurement of thiocyanate and nitrate transport may be of particular interest because dietary consumption and environmental exposure lead to elevated plasma concentrations in the hundred micromolar range that produce detectable changes in cellular YFP–H148Q/I152L fluorescence. Gastric and salivary gland NIS is thought to contribute to the entero-salivary recycling of thiocyanate and nitrate, and transport by placental and mammary gland NIS may lead to exposure of the fetus and nursing infant, respectively, to these environmental anions. Finally, YFP–H148Q/I152L may be useful to identify other mammalian and nonmammalian anion transporters (e.g., chlorate/nitrate transporters in plant cells), and the generation of further variants with increased sensitivities to specific anions may provide tools to investigate their physiological function as well as the health-related consequences of environmental exposure.

Acknowledgments

This work was supported by Grants from the Italian Ministry of University and Research (MIUR, PRIN2007), the University of Bologna Ricerca Fondamentale Orientata (RFO ex 60%) to K.J.R. and a postdoctoral fellowship from the University of Bologna to J.D.B.

References

[1] L.J.V. Galietta, P.M. Haggie, A.S. Verkman, Green fluorescent protein-based halide indicators with improved chloride and iodide affinities, FEBS Lett. 499 (2001) 220–224.
[2] L.J.V. Galietta, S. Jayaraman, A.S. Verkman, Cell-based assay for high-throughput quantitative screening of CFTR chloride transport agonists, Am. J. Physiol. 281 (2001) C1734–C1742.
[3] W. Kruger, D. Gilbert, R. Hawthorne, D.H. Hryciw, S. Frings, P. Poronnik, J.W. Lynch, A yellow fluorescent protein-based assay for high-throughput screening of glycine and GABAA receptor chloride channels, Neurosci. Lett. 380 (2005) 340–345.
[4] N. Pedemonte, G.L. Lukacs, K. Du, E. Caci, O. Zegarra-Moran, L.J. Galietta, A.S. Verkman, Small-molecule correctors of defective ΔF508–CFTR cellular processing identified by high-throughput screening, J. Clin. Invest. 115 (2005) 2564–2571.
[5] K. Berglund, W. Schleich, H. Wang, G. Feng, W.C. Hall, T. Kuner, G.J. Augustine, Imaging synaptic inhibition throughout the brain via genetically targeted Clomeleon, Brain Cell. Biol. 36 (2008) 101–118.
[6] R. De La Fuente, W. Namkung, A. Mills, A.S. Verkman, Small-molecule screen identifies inhibitors of a human intestinal calcium-activated chloride channel, Mol. Pharmacol. 73 (2008) 768–778.
[7] O. Markova, M. Mukhtarov, E. Real, Y. Jacob, P.J. Bregestovski, Genetically encoded chloride indicator with improved sensitivity, Neurosci. Methods 170 (2008) 67–76.
[8] O. Dohan, A. De la Vieja, V. Paroder, C. Riedel, M. Artani, M. Reed, C.S. Ginter, N. Carrasc, The sodium/iodide symporter (NIS): characterization, regulation, and medical significance, Endocr. Rev. 24 (2003) 48–77.
[9] J. Van Sande, C. Massart, R. Beauwens, A. Schoutens, S. Costagliola, J.E. Dumont, J. Wolff, Anion selectivity by the sodium iodide symporter, Endocrinology 144 (2003) 247–252.
[10] S. Eskandari, D.D. Loo, G. Dai, O. Levy, E.M. Wright, N. Carrasco, Thyroid Na^+/I^-symporter: mechanism, stoichiometry, and specificity, J. Biol. Chem. 272 (1997) 27230–27238.
[11] J.B. Wyngaarden, B.M. Wright, P. Ways, The effect of certain anions upon the accumulation and retention of iodide by the thyroid gland, Endocrinology 50 (1952) 537–549.
[12] J. Wolff, Transport of iodide and other anions in the thyroid gland, Physiol. Rev. 44 (1964) 45–90.
[13] R. Ihalin, V. Loimaranta, J. Tenovuo, Origin, structure, and biological activities of peroxidases in human saliva, Arch. Biochem. Biophys. 445 (2006) 261–268.
[14] T.M. Vogt, S. Selvin, G. Widdowson, S.B. Hulley, Expired air carbon monoxide and serum thiocyanate as objective measures of cigarette exposure, Am. J. Public Health 67 (1977) 545–549.
[15] J.O. Lundberg, E. Weitzberg, M.T. Gladwin, The nitrate–nitrite–nitric oxide pathway in physiology and therapeutics, Nat. Rev. Drug Discov. 7 (2008) 156–167.
[16] D.M. Manassaram, L.C. Backer, D.M. Moll, A review of nitrates in drinking water: maternal exposure and adverse reproductive and developmental outcome, Environ. Health Perspect. 114 (2006) 320–327.
[17] National Research Council, Health Implications of Perchlorate Ingestion, National Academies Press, Washington, DC, 2005.
[18] S.A. Snyder, B.J. Vanderford, D.J. Rexing, Trace analysis of bromate, chlorate, iodate, and perchlorate in natural and bottled waters, Environ. Sci. Technol. 39 (2005) 4586–4593.
[19] E.N. Pearce, L.E. Braverman, Environmental pollutants and the thyroid, Best Pract. Res. Clin. Endocrinol. Metab. 23 (2009) 801–813.
[20] J. Meller, W. Becker, The continuing importance of thyroid scintigraphy in the era of high-resolution ultrasound, Eur. J. Nucl. Med. Mol. Imaging 29 (2002) S425–S438.
[21] E. Dadachova, A. Nguyen, E.Y. Lin, L. Gnatovskiy, P. Lu, J.W. Pollard, Treatment with rhenium-188-perrhenate and iodine-131 of NIS-expressing mammary cancer in a mouse model remarkably inhibited tumor growth, Nucl. Med. Biol. 32 (2005) 695–700.
[22] T. Petrich, L. Quintanilla-Martinez, Z. Korkmaz, E. Samson, H.J. Helmeke, G.J. Meyer, W.H. Knapp, E. Pötter, Effective cancer therapy with the α-particle

emitter [211At]astatine in a mouse model of genetically modified sodium/iodide symporter-expressing tumors, Clin. Cancer Res. 12 (2006) 1342–1348.
[23] G. Dai, O. Levy, N. Carrasco, Cloning and characterization of the thyroid iodide transporter, Nature 379 (1996) 458–460.
[24] P.A. Smanik, Q. Liu, T.L. Furminger, K. Ryu, S. Xing, E.L. Mazzaferri, S.M. Jhiang, Cloning of the human sodium iodide symporter, Biochem. Biophys. Res. Commun. 226 (1996) 339–345.
[25] N. Tran, L. Valentín-Blasini, B.C. Blount, C.G. McCuistion, M.S. Fenton, E. Gin, A. Salem, J.M. Hershman, Thyroid-stimulating hormone increases active transport of perchlorate into thyroid cells, Am. J. Physiol. Endocrinol. Metab. 294 (2008) E802–E806.
[26] K.J. Rhoden, S. Cianchetta, V. Stivani, C. Portulano, L.J.V. Galietta, G. Romeo, Cell-based imaging of sodium iodide symporter activity with the yellow fluorescent protein variant YFP–H148Q/I152L, Am. J. Physiol. 292 (2007) C814–C823.
[27] K.J. Rhoden, S. Cianchetta, S. Duchi, G. Romeo, Fluorescence quantitation of thyrocyte iodide accumulation with the yellow fluorescent protein variant YFP–H148Q/I152L, Anal. Biochem. 373 (2008) 239–246.
[28] S. Cianchetta, J. Di Bernardo, G. Romeo, K.J. Rhoden, Perchlorate transport and inhibition of the sodium iodide symporter measured with the yellow fluorescent protein variant YFP–H148Q/I152L, Toxicol. Appl. Pharmacol. 243 (2010) 372–380.
[29] F.S. Ambesi-Impiombato, L.A. Parks, H.G. Coon, Culture of hormone-dependent functional epithelial cells from rat thyroids, Proc. Natl. Acad. Sci. USA (1980) 3455–3459.
[30] S. Jayaraman, P. Haggie, R.M. Wachter, S.J. Remington, A.S. Verkman, Mechanism and cellular applications of a green fluorescent protein-based halide sensor, J. Biol. Chem. 275 (2000) 6047–6050.
[31] R.M. Wachter, D. Yarbrough, K. Kallio, S.J. Remington, Crystallographic and energetic analysis of binding of selected anions to the yellow variants of green fluorescent protein, J. Mol. Biol. 301 (2000) 157–171.
[32] S.J. Weiss, N.J. Philp, E.F. Grollman, Iodide transport in a continuous line of cultured cells from rat thyroid, Endocrinology 114 (1984) 1090–1098.
[33] S.Y. Chow, D.M. Woodbury, Water and electrolyte distribution in rat and guinea-pig thyroid glands, J. Endocrinol. 50 (1971) 561–576.
[34] R.M. Wachter, S.J. Remington, Sensitivity of the yellow variant of green fluorescent protein to halides and nitrate, Curr. Biol. 9 (1999) R628–R629.
[35] S. Kosugi, N. Sasaki, N. Hai, H. Sugawa, N. Aoki, C. Shigemasa, T. Mori, A. Yoshida, Establishment and characterization of a Chinese hamster ovary cell line, CHO-4J, stably expressing a number of N^+/I^- symporters, Biochem. Biophys. Res. Commun. 227 (1996) 94–101.
[36] L.S. Zuckier, O. Dohan, Y. Li, C.J. Chang, N. Carrasco, E. Dadachova, Kinetics of perrhenate uptake and comparative biodistribution of perrhenate, pertechnetate, and iodide by NaI symporter-expressing tissues in vivo, J. Nucl. Med. 45 (2004) 500–507.
[37] M. Tonacchera, A. Pinchera, A. Dimida, E. Ferrarini, P. Agretti, P. Vitti, F. Santini, K. Crump, J. Gibbs, Relative potencies and additivity of perchlorate, thiocyanate, nitrate, and iodide on the inhibition of radioactive iodide uptake by the human sodium iodide symporter, Thyroid 14 (2004) 1012–1019.
[38] J. Wolff, Perchlorate and the thyroid gland, Pharmacol. Rev. 50 (1998) 89–105.
[39] E.A. Merrill, R.A. Clewell, P.J. Robinson, A.M. Jarabek, J.M. Gearhart, T.R. Sterner, J.W. Fisher, PBPK model for radioactive iodide and perchlorate kinetics and perchlorate-induced inhibition of iodide uptake in humans, Toxicol. Sci. 83 (2005) 25–43.